

# Electromagnetic Wave Source Visualization System with Lüneburg Lens

Aya Ohmae, Isao Hoda, Umberto Paoletti, Wen Li, Takashi Suga and Hideki Osaka

Yokohama Research Laboratory  
Hitachi Ltd.  
Yokohama, Japan  
aya.ohmae.xh@hitachi.com

**Abstract**—A new real-time and high resolution electromagnetic wave source visualization system is presented. The system can determine the angle of incidence and visualize the wave source by combining a Lüneburg lens and an electromagnetic band gap (EBG) absorber. The Lüneburg lens is used to physically separate the different direction incident wave and focus them into the different focal points on the lens surface. The every element of EBG absorber is coincide with a different focal point on the lens surface, the intensity and angle information of the incident wave can be obtained based on the absorbed power and position of the corresponding sensor element. The estimated angular resolution is  $\pm 0.75$  degree theoretically and the system sensitivity is  $-90$ dBm at 2.45GHz. The results have been confirmed by simulations and prototype evaluations.

**Keywords**—Electromagnetic Band Gap; Lüneburg Lens; Electromagnetic wave source visualization;

## I. INTRODUCTION

Locating the electromagnetic wave sources from electronic, communication and industrial equipments is an important issue in electromagnetic comparability (EMC) field. Being in a smaller space and investigating the smaller electronic device, near field scanning is a popular technique. For the larger space and object, it is difficult to scan all of space because of the complicated scanning system and the longer measurement times required.

Direction-of-arrival (DOA) estimation is a good choice and has attracted a lot of attention<sup>[1]</sup>. Most microwave direction finding system is based on antenna array with a sophisticated algorithm like multiple signal classification (MUSIC)<sup>[2]</sup>, Root-MUSIC<sup>[3]</sup> or estimation of signal parameters via rotational invariance technique (ESPRIT)<sup>[4]</sup>. To achieve high resolution in the incident angle from far field, the complicated signal processing algorithms are required. The cost, speed and power consumption associated with the hardware and software requirement could be strict, especially for portable and real-time applications.

A Lüneburg lens<sup>[5]</sup> with Photonic Sensors<sup>[6]</sup> or Power Detectors<sup>[7]</sup> is another DOA techniques without sophisticated algorithm. The lens has unique characteristic. Every point on the surface of the lens is the focal point of a plane wave incident from the opposite side. The photonic sensor or power detector is used to detect the incident wave which

corresponds to the focal point. However, a number of discrete sensors or detectors must be mounted on the lens surface in order to get higher angle resolution. Pre-calibration and signal processing can reduce the detectors numbers but will lose the real-time property. This paper proposes a new high resolution electromagnetic wave localization technique with Lüneburg lens and electromagnetic band gap (EBG) absorber<sup>[8], [9]</sup>. The effect of the proposed technique has been confirmed by simulation and prototype evaluations.

## II. CONCEPT OF ELECTROMAGNETIC WAVE VISUALIZATION

The proposed system is mainly composed of a Lüneburg lens and a electromagnetic band gap absorber. The Lüneburg lens is used to physically separate the different direction incident wave and focus the same direction wave into a focal point on the lens surface. The EBG absorber is employed as a compact 2D sensor array whose every element is coincide with a different focal point on the lens surface, the intensity and angle information of the incident wave can be obtained based on the absorbed power and position of the corresponding sensor element. Therefore, the proposed system can distinguish the different direction incident wave and measure them by the different sensor elements at the same time. By superimposing the camera image and the distribution of sensor data, the system could real-time visualize the wave source position like a “electromagnetic wave camera.” The architecture and the target specification of the proposed system are shown in Fig 1 and Table I respectively.

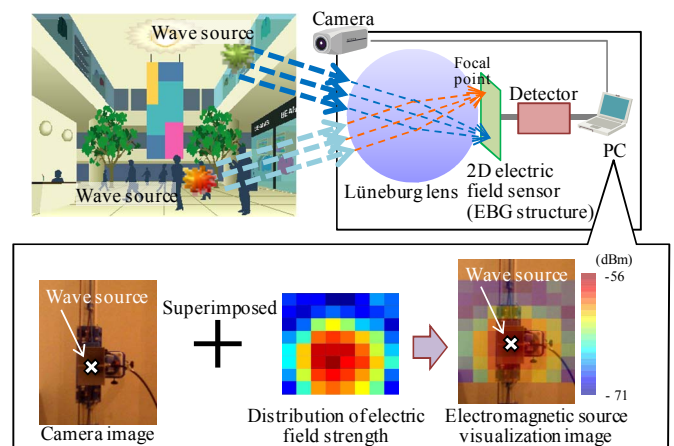


Fig 1. Concept of new wave source visualization system

TABLE I. TARGET SPEC

|                               |                 |
|-------------------------------|-----------------|
| Frequency                     | 2.45 GHz        |
| Estimated resolution of angle | $\pm 0.75$ deg. |
| Sensitivity                   | -90 dBm         |

### A. Luneburg Lens

In our new electromagnetic wave source visualization system, a Luneburg lens is adopted because it has two important functions: one is to physically distinguish the different directions of incident waves and focus them to different focal points. Another one is to amplify the incident wave by the focusing function. Fig 2. shows the structure of the lens. The Luneburg lens is a spherical structure with gradually changing relative permittivity. The relative permittivity of the lens can be described by the following formula.

$$\epsilon_r(r) = 2 - \left(\frac{r}{R}\right)^2 \quad (1)$$

$R$  : radius of the lens,  $r$  : distance from center of the lens  
 $\epsilon_r$  : relative permittivity at  $r$

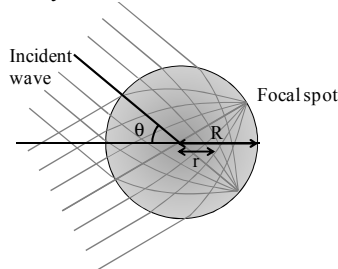


Fig 2. Luneburg Lens

Ideally, it is desirable to gradually change the relative permittivity. However, it is too difficult to control a continual change of material permittivity. One realistic option is the layered structure whose relative permittivity of every layer is changed slowly. Fig 3 shows the permittivity of such a layered model.

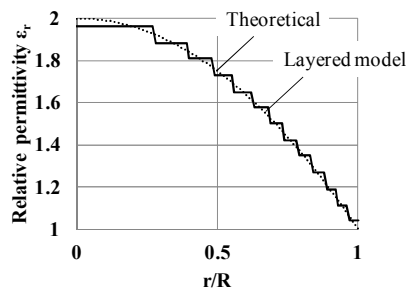


Fig 3. Permittivity of Luneburg lens

Fig 4 shows the simulation result of a 13 layered Luneburg lens. The relative permittivity is designed as Fig 3 and the lens radius is 400 mm. The result shows the power gain at every focal point of the lens surface when there is an incident wave of 0 or 10 degree from the opposite side. The lens focuses the power of the incident wave on the corresponding focal point and has a gain of 20dB.

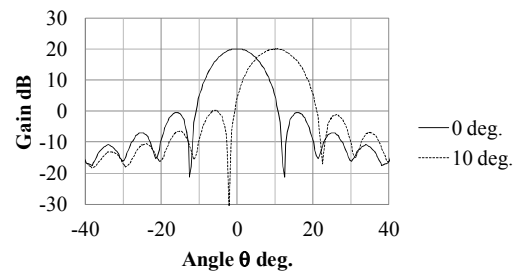


Fig 4. Gain of Luneburg Lens

### B. Electromagnetic Band Gap Absorber

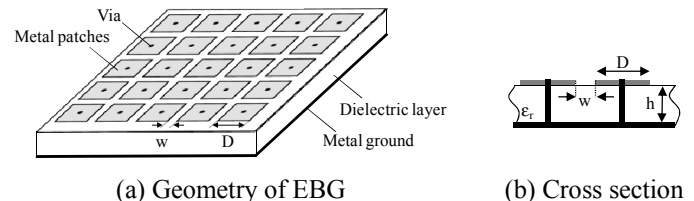
In order to decrease the numbers of the discrete antennas or sensors which increase the complication of the whole system, a compact 2D sensor is designed based on the mushroom type EBG absorber. The mushroom type EBG structure is well known as one of the artificial high-impedance surface materials. The resonance frequency at which the surface exhibits the high-impedance feature is decided by the size of the periodical structure. Fig 5 shows an example of the mushroom type EBG structure. The parasitic capacitance  $C$  and parasitic inductance  $L$  of the structure can be described approximately by the following formulas [10]-[12].

$$C = \frac{D\epsilon_0(\epsilon_r + 1)}{\pi} \cosh^{-1}\left(\frac{D+w}{w}\right) \quad (D \ll \lambda, w \ll D) \quad (2)$$

$$L = \mu_0 h \quad (h \ll D) \quad (3)$$

The resonant frequency is described as a simple equation.

$$f = \frac{1}{2\pi\sqrt{LC}} \quad (4)$$



(a) Geometry of EBG

(b) Cross section

Fig 5. Structure of mushroom type EBG

In addition, the EBG absorber has resistive components for absorbing the incident wave. At the resonant frequency, the mushroom structure exhibits the high impedance feature and the incident wave is absorbed by the resistive components which are matched with the incident wave impedance. The power of the absorbed incident wave can be measured by connecting each resistive component to a detecting circuit.

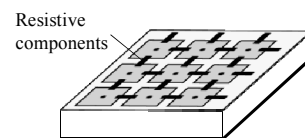


Fig 6. Geometry of EBG absorber

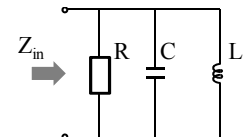


Fig 7. Equation circuit of EBG absorber

TABLE II. shows the parameters of EBG absorber designed for 2.45GHz. Each patch size is decided to satisfy the conditions:  $D \ll \lambda$  (122.45mm) and  $w, h \ll D$ . Furthermore, in order to achieve the higher resolution, the patch size  $D$  is designed shorter than the tenth part of the wavelength. The theoretical resonant frequency based on the designed size is 4.98GHz ( $C$  and  $L$  is 0.58pF and 1.76nH). For moving the resonant frequency to 2.45GHz, a lumped capacitance  $C_{add}=1.81\text{pF}$  is added between the patches according the following simple formula,

$$f = \frac{1}{2\pi\sqrt{L(C+C_{add})}} = 2.45\text{GHz} \quad (5)$$

TABLE II. PARAMETERS OF EBG ABSORBER

|                                      |                |
|--------------------------------------|----------------|
| Patch size $D$                       | 10mm           |
| Patch distance $w$                   | 0.5mm          |
| Thickness $h$                        | 1.4mm          |
| Additional capacitance $C_{add}$     | 1.55pF         |
| Resistive component $R$              | 377 $\Omega$   |
| Dielectric permittivity $\epsilon_r$ | 4.5            |
| Number of patches                    | 30 $\times$ 31 |

Fig 8 shows the reflection characteristic which is simulated by CST MW STUDIO. The resonant frequency is lower than 2.45GHz with  $C_{add}=1.81\text{pF}$  because of the approximated error. The resonance frequency after fine adjustment with  $C_{add}=1.55\text{pF}$  is 2.45GHz.

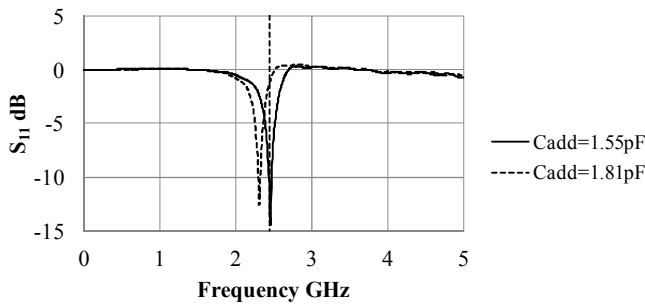


Fig 8. Reflection characteristic of EBG absorber

### III. SIMULATION RESULTS

In this section, the proposed method is confirmed through simulation. Fig 9 shows the simulation model of the proposed method. The center of EBG sensor is located on the 0 degree focal point of a 13 layered Lüneburg lens. The angle range of the incident wave is from 0 to 20 degree. The parameters of EBG absorber are same as TABLE II.

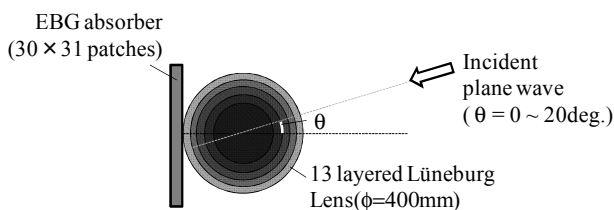


Fig 9. Simulation model

The simulation results with the incident angle of 0 degree and 10 degree are shown in Fig 10(a) and Fig 10(b), respectively. Each result shows the power map of the resistive components whose positions are coincide with the different incident direction. The angle of the incident wave can be obtained according to the position of the maximum power level of the map.

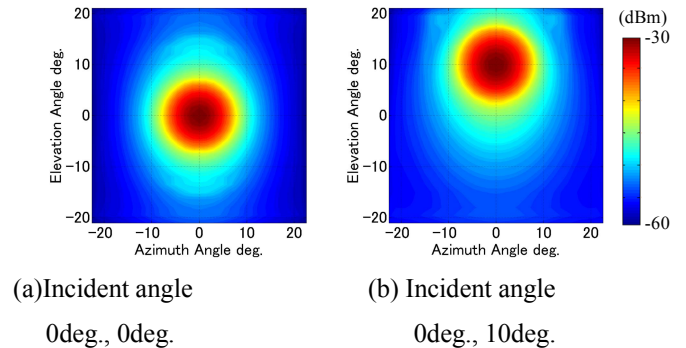


Fig 10. Visualization result of electric field

The estimation error of angle based on the simulation is shown in Fig 11. The error is due to the discrete sensor position decided by the patch size and patch distance. The expected maximum estimation error is  $\pm 0.75$  degree. The error limits the resolution and can be improved by reducing the patch size.

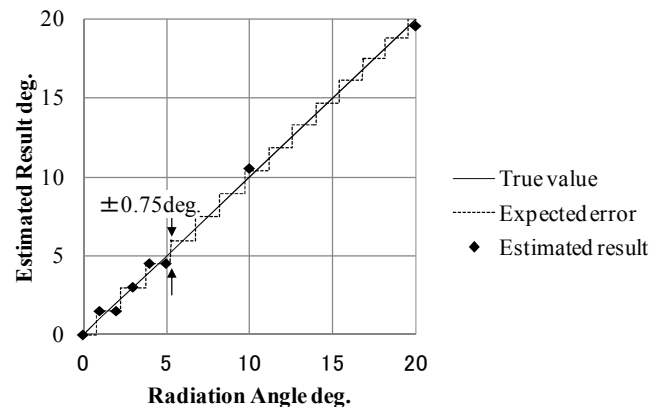


Fig 11. Estimation error of angle

### IV. EXPERIMENTAL RESULTS

As a proof-of-concept demonstration, a trial system is studied and verified by an experiment. Fig 12 and Fig 13 show the experimental setup in an anechoic chamber. Most parameters of EBG absorber are same as TABLE II, except that  $R=360 \Omega$ ,  $C_{add}=1.3\text{pF}$ , Number of patches=30 $\times$ 30 and FR4 is used. In this experiment, 8 $\times$ 8 resistive components on the center-section of EBG absorber are connected to a detecting circuit. The radio frequency signal is converted to DC voltage by the received signal strength indicator (RSSI). Being different with the general ideal Lüneburg lens whose focal points are on the lens surface, the focal points of the trial Lüneburg lens are on a virtual spherical surface 70mm behind the lens surface. It is convenient to locate the center of EBG sensor on the 0 degree focal point of the Lüneburg lens

( $R=400\text{mm}$ ). Horn antenna is set 3 meters away from EBG sensor as an electromagnetic wave source. The antenna height and angle is changed while keeping the distance from the lens. A camera is set near the lens for taking the picture of the measuring object.

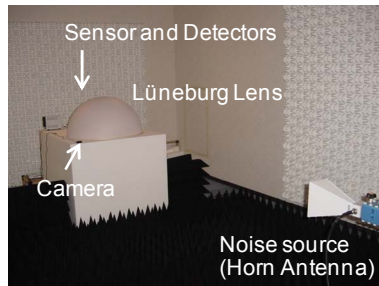


Fig 12. Experimental setup in anechoic chamber

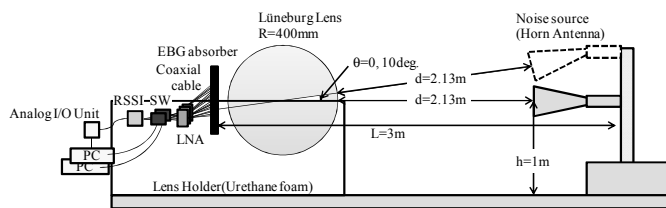
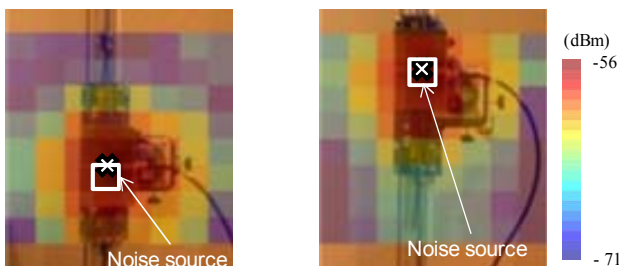


Fig 13. Experimental setup of electromagnetic wave visualization

The measured power map and the picture of the measuring object are overlapped on PC. Fig 14 shows the measuring results at the different incident angle of 0 degree and 10 degree, respectively. The angle of incident wave can be obtained according to the different position of the maximum power level in Fig 14(a) and Fig 15(b), respectively. The white 'x' mark shows the expected position coinciding with the incident angle, the white square shows the measured position.



(a) Incident angle = 0deg. (b) Incident angle = 10deg.

Fig 14. Visualization result of electric field

Fig 15 shows the measurable power range of the electromagnetic wave visualization system. The incident power level on Lens surface is estimated from the output level of signal generator, horn antennas gain and distance between the antenna and lens surface. The minimum power level on Lens surface corresponded to the linear output range is  $-90\text{ dBm}$ , which is lower than the EMC regulation at  $2.45\text{GHz}$ . Therefore, the system can localize electromagnetic wave sources required in EMC field.

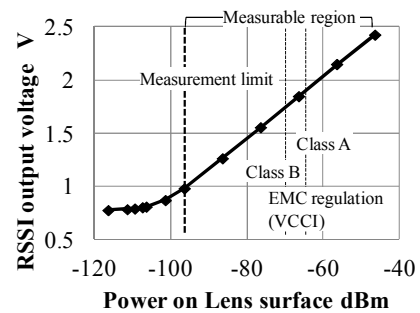


Fig 15. Measurement limit of the electromagnetic wave visualization system

## V. CONCLUSION

A new electromagnetic wave source visualization system by combining a Lüneburg lens and a compact 2D EBG sensor array was studied. The proposed system can localize electromagnetic wave source without complicated signal processing algorithm and a number of discrete hardware elements as general DOA system. The estimated angular resolution is  $\pm 0.75\text{degree}$  theoretically and the system sensitivity is  $-90\text{dBm}$  at  $2.45\text{GHz}$ . The results have been confirmed by simulations and prototype evaluations. The expansion of a wider frequency band is a future study.

## REFERENCES

- [1] L.C. Godara, "Application of antenna arrays to mobile communications. II. Beam-forming and direction-of-arrival considerations" *Proc. IEEE*, Vol. 85, no. 8, pp. 1195-1245, 1997
- [2] R. O. Schmidt, "Multiple Emitter Location and Signal Parameter Estimation," *IEEE Trans., Antennas & Propagation*, Vol. AP-34, NO. 3, pp. 276-280, March 1986
- [3] B. D. Rao, K. V. S. Hari, "Performance Analysis of Root-MUSIC," *IEEE Trans. Acoustics. Speech and Signal Processing*, Vol. 37, No. 12, pp. 1939-1949, December 1989
- [4] R. Roy, T. Kailath, "ESPRIT-Estimation of Signal Parameters Via Rotational Invariance Techniques," *IEEE Trans. Acoustics. Speech and Signal Processing*, Vol. 37, No. 7, pp.984-995, July 1989
- [5] R. K. Luneburg, "Mathematical Theory of Optics," pp. 182-188, University of California Press, 1964
- [6] Hilliard, D, Mensa, D, "Luneburg lens antenna with photonic sensors", *Antennas and Propagation Society International Symposium*, 1992.
- [7] M. Liang, X. Yu, R. S. Gracia, W. R. Ng, M. E.Gehm, H. Xin, "Direction of arrival estimation using Luneburg lens," *IEEE MTT-S International, Microwave Symposium Digest*, June 2012
- [8] S. Yagitani, K. Katsuda, M. Nojima, Y. Yoshimura, H. Sugiura, "Imaging Radio-Frequency Power Distributions by an EBG Absorber," *IEICE Trans., Communication*, Vol. 2011, No. 8, pp.2306-2315, 2011
- [9] S. Yagitani, K. Katsuda, R. Tanaka, M. Nojima, Y. Yoshimura, H. Sugiura, "A Tunable EBG Absorber for Radio-Frequency Power Imaging," *XXXth URSI General Assembly and Scientific Symposium*, 2011
- [10] S. Tratyakov, "Analytical Modeling in Applied Electromagnetics," pp223, 2003
- [11] J. M. Bell, M. F. Iskander, "Equivalent Circuit Model of an Ultrawideband Hybrid EBG/Ferrite Structure," *IEEE Antennas and Wireless Propagation Letters*, Vol. 7 2008, pp573-576, 2008
- [12] D. F. Sevenpiper, "High-Impedance Electromagnetic Surfaces," Doctoral dissertation of University of California Los Angeles, pp43, 1999